Mineralogical Magazine, February 1999, Vol. 63(1), pp. 111–122

Fluid circulation in the Apuane Alps core complex: evidence from extension veins in the Carrara marble

P. COSTAGLIOLA[1], M. BENVENUTI[2,3], C. MAINERI[2,3], P. LATTANZI[3,4] AND G. RUGGIERI[5]

[1] Museo di Mineralogia e Litologia, Università di Firenze, Via La Pira 4, I-50121, Firenze, Italy
[2] Dipartimento di Scienze della Terra, Università di Firenze, Via La Pira 4, I-50121, Firenze, Italy
[3] CNR C.S. Minerogenesi e Geochimica Applicata, Via La Pira 4, I-50121, Firenze, Italy
[4] Dipartimento di Scienze della Terra, Università di Cagliari, via Trentino 51, I-09127, Cagliari, Italy
[5] CNR, Istituto Internazionale per le Ricerche Geotermiche, Piazza Solferino 2, I-56126, Pisa, Italy

ABSTRACT

In the Apuane Alps (AA) metamorphic core complex, syn-metamorphic mineral deposits are mainly restricted to extensional shear zones in the Lower Plate Palaeozoic basement. By contrast, the extension structures at upper levels, such as the detachment fault, that are typically the seat of fluid circulation and mineralization in other core complexes, are barren in the AA. Extension veins hosted by the Jurassic Carrara marbles are among the few examples of (minor) mineralization located in the upper levels of the AA core complex. Calcite–dolomite geothermometry and fluid inclusion data suggest that the mineralizing process in these veins began under pressure (P)-temperature (T) conditions close to the metamorphic peak (about 400°C, 3 kbar). Progressive cooling and mixing between metamorphic and late stage meteoric fluids were probably responsible for most of the mineral deposition. Batches of relatively saline fluids presumably resulted from interaction with evaporitic levels located along the detachment fault. In agreement with previous estimates, fluid inclusion constraints on the P–T synmetamorphic path of the AA suggest a relatively rapid cooling of the core complex as a result of uplift. However, the maximum estimated geothermal gradient (about 35°C/km) is considerably lower than in other core complexes, where large-scale hydrothermal circulation was associated with extension and uplift. Hence, in the AA, fluid circulation at shallow levels and mixing among fluids of different origin were not favoured, thus precluding the formation of mineral deposits along major extensional structures.

KEYWORDS: fluid inclusions, core complex, uplift path, extensional veins, Carrara marble, Northern Apennines.

Introduction

IN the AA core complex (Carmignani and Kligfield, 1990), a number of mineral deposits are associated with syn- to late- metamorphic tectonic features (Lattanzi *et al.*, 1994; Costagliola *et al.*, 1998; and references therein). Evidence of synchronism between metamorphism, extension and (mineralizing) fluid circulation is a rather common feature in core complexes (Beaudoin *et al.*, 1991, 1992; Kerrich, 1987; Kyser and Kerrich, 1990; Doblas *et al.*, 1988; Spencer and Welty, 1986; Smith *et al.*, 1991). However, in contrast to other core complexes, the fluid circulation in the AA was apparently restricted to the lower levels of the 'Lower Plate', whereas the detachment fault and the 'Upper Plate' do not host any deposit. Recently, Hodgkins and Stewart (1994) found some evidence of fluid circulation along the AA detachment fault during extension and uplift, represented by fluid inclusions hosted in minerals cementing the fault breccia. Additional evidence of fluid circulation in the middle and upper levels of the AA complex are represented by (minor) extension veins, hosted in particular in the Carrara marbles, belonging to the Mesozoic cover of the basement sequence. In this paper, we investigate the fluid circulation in these veins, using fluid inclusions and the calcite geothermometer. Based

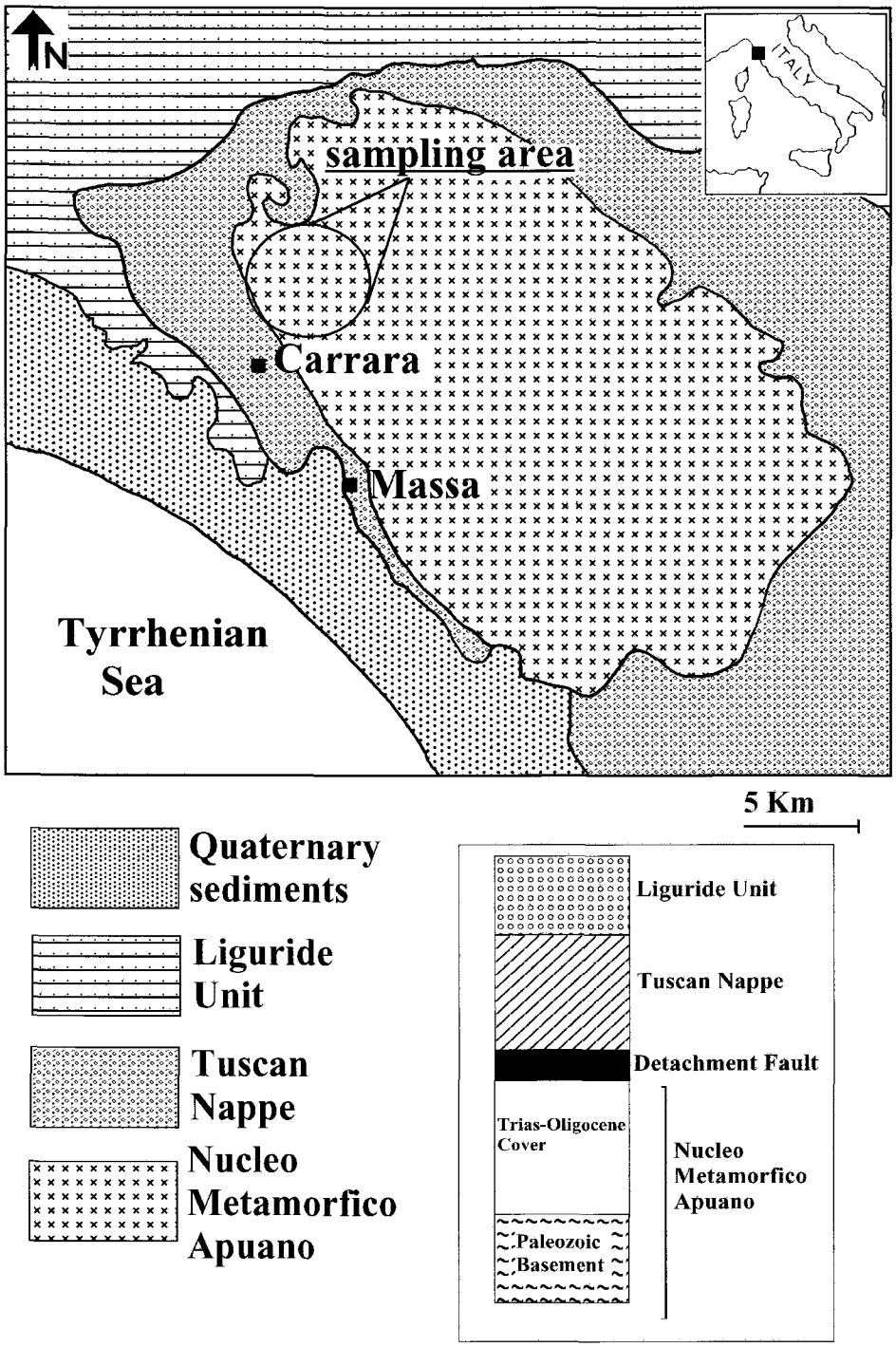

. Simplified geological map of the Apuane Alps. At the right-bottom side, the tectono-stratigraphic column of the Apuane Alps. The thickness of the formations and Units is not to scale.

on these and previous data, we discuss the uplift path of the AA and the nature of the hydrothermal fluids that migrated in the crust during thinning and extension. The inferred hydrologic regime during mineral deposition in extension structures is compared with those encountered in mineralized core complexes and extensional areas.

Geological setting

Regional geology

The Apuane Alps (AA) are a tectonic window located in the northernmost tip of the Tuscan Apennines. The lowermost Unit is represented by the Nucleo Metamorfico Apuano (NMA), which comprises a Palaeozoic basement and a Triassic to Oligocene cover, that were metamorphosed under greenschist facies conditions (T = 350–450°C; P = 3.0–4.0 kbar; Carmignani and Kligfield, 1990; Fig. 1). The NMA is overlain by the non-metamorphic Tuscan Nappe and Liguride Unit. The NMA and Tuscan Nappe are separated by a brecciated zone, interpreted as the detachment fault of the AA core complex (Carmignani and Kligfield, 1990). Two major deformation phases affected the AA area: a compressional phase (D_1), responsible for the emplacement of the Tuscan Nappe and the overlying Liguride Unit over the AA zone, and an extensional phase (D_2), dated at 27 and 12–8 Ma, respectively (Kligfield *et al.*, 1986). Carmignani and Kligfield (1990) proposed that several shear zones developed during the D_2 phase in response to the gravitational collapse of the AA, thereby accommodating part of its extension. Tectonic extension was also accomplished by brecciation of evaporitic rocks (Calcare Cavernoso, Trias) at the base of the Tuscan Nappe, which acted as a glide horizon, (Carmignani and Kligfield, 1990).

Mineral deposits of the AA comprise a number of Fe-Ba(Pb, Zn, Ag), Pb-Zn(Ag), Hg, and Cu-Fe syntectonic vein deposits, hosted by the AA basement rocks (Lattanzi *et al.*, 1994; Benvenuti *et al.*, 1995; Costagliola *et al.*, 1995, 1998). At least a part of them was emplaced along syn-D_2 shear zones connected with the extensional phase of the AA core complex.

Extension veins in the Carrara marble

The Carrara Marble formation (Hettangian) is a part of the Mesozoic cover of the NMA (Fig. 1). It crops out extensively near Carrara, where a major quarrying activity is documented since ancient times. Quartz-calcite veins and voids are common within white, coarse-grained calcite levels, the 'Macchia Bianca' (MB), thought to be of sedimentary origin (Bracci *et al.*, 1978). MB has a thickness ranging 1–15 cm, and shows fairly constant dip and strike (40–60° and 240° respectively). It is generally undeformed, although, locally, folds have been observed. Fractures in the MB (Fig. 2) follow an *en-echelon* array, with shapes ranging from sigmoidal to irregular, and are partially or completely filled by calcite, quartz, and a large variety of other minerals (more than 70 mineral species, mainly represented by sulphides, sulphosalts, carbonates and halides; Franzini *et al.*, 1992 and references therein; Crisci *et al.*, 1997). The geometry of the fracture arrays indicate a sense of shear from NE toward SW, compatible with the D_2 kinematics of this area (Carmignani and Kligfield, 1990; Carmignani *et al.*, 1992; see also Orlandi *et al.*, 1996).

The studied samples were collected in the Carrara area (Fig. 1), and currently belong to the collections of the Museo di Mineralogia, Università di Firenze. The main minerals are represented by calcite and dolomite, often intergrown (in equilibrium textures) with accessory quartz, fluorite and pyrite. Calcite and quartz frequently occupy the vein walls (hereafter 'early generation'). These two minerals, especially calcite, may also occur as late stage overgrowths onto preexisting minerals (hereafter 'late generation').

Results

Analytical techniques

All analyses were performed with facilities of the Museo di Storia Naturale, Dipartimento di

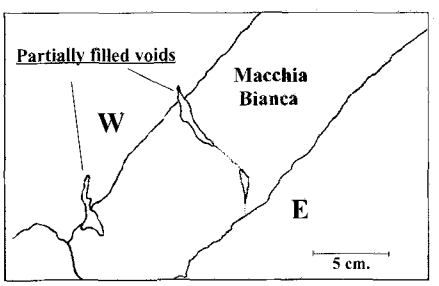

FIG. 2. Sketch of the veins hosted by Macchia Bianca.

Scienze della Terra, and CNR C.S. Minerogenesi e Geochimica Applicata, Firenze. Samples were prepared as doubly polished thin sections having a thickness of about 0.7 mm. Calcite analyses were performed by using a JEOL JXA 8600 Superprobe electron microprobe. Dolomite, calcite, ilmenite and rhodonite standards were used for Mg, Ca, Fe, Mn and Si. Beam operating conditions were 15 kV, 10 nA with a diameter of approximately 20 μm. Microthermometric measurements of fluid inclusions were performed with a U.S.G.S.-type gas-flow heating-freezing stage. The thermocouple of the stage was calibrated using suitable standards. Replicate measurements were made on about 20% of the inclusions. Homogenization and ice melting temperatures are generally reproducible within 2°C (in the range 0–550°C) and 0.3°C (in the range −100–0°C), respectively. Raman analyses of gas phase in fluid inclusions were carried out using a Jobin-Yvon S 3000 spectrograph equipped with an Ar+ laser source as exciting radiation, a CCD type detector, and an Olympus BH 2 microscope.

Fluid inclusions

Inclusions suitable for microthermometric studies were observed only in quartz. They are two-phase inclusions, liquid-rich at room temperature, having mostly ellipsoidal, subhedral or euhedral morphology. Their average size is of about 20 μm. Some inclusions, displaying an irregular shape and necking-down textures, were not considered in this study.

Inclusions may occur either isolated, or grouped along planes; the former have been considered as primary, and the latter as secondary. Textures clearly related to post-entrapment changes (cf. Sterner and Bodnar, 1989; Vitik and Bodnar, 1995) were not observed. Low-temperature behaviour and Raman microspectroscopy suggest that CO_2 is absent in most of the fluid inclusions; Raman microspectroscopy also revealed no other compounds, such as CH_4, N_2, H_2S, in the gas phase. The rare occurrence of CO_2 was neglected in the following calculations. Ice first melting temperatures were generally around −23°C, suggesting that the trapped fluids mainly belong to the H_2O-NaCl-KCl system. Salinity of the liquid phase was estimated from the melting temperature of ice using the data of Bodnar (1993). Upon heating all the inclusions homogenize to the liquid phase.

Overall salinity and temperature of homogenization (T_h) values are in the range of 1.5–25 wt.% NaCl eq. and 130–240°C, respectively. In a salinity *vs.* T_h plane (Fig. 3), the data plot as an overturned V. The extremes of the V correspond to three hypothetical end-member fluids that we have indicated in Fig. 3 as A, B and C, respectively. The 'A' end-member is characterized by T_h and salinity of about 225°C and 12.5 wt.% NaCl, respectively. It occurs within primary and secondary inclusions with a negative crystal shape, mostly hosted by the early generation of quartz (Table 1). Two linear arrays of data depart from A and point to B and C end-member fluids (Fig. 3), characterized by lower T_h and variable salinities. In particular, in B fluids salinities reach values as low as 1.5 wt.% NaCl, with T_h down to about 130°C. The corresponding inclusions are generally secondary, but may be primary in the late generation of quartz. The A–C trend comprises a relatively smaller amount of data, with C end-member values showing the highest salinity of 25 wt.% NaCl eq. and a corresponding T_h of about 160°C. The inclusions

TABLE 1. Summary of fluid inclusion data in quartz from extension veins in the Carrara Marble. See text and Fig. 3 for explanation

Fluid Type phase	Timing of the host (quartz)	Fluid inclusion texture	T_h (°C)	Salinity (wt.% NaCl eq.)
A	Early	Primary or secondary	225*	12.2*
B and A–B trend	Early/late	Secondary, or sometimes primary in the late quartz	130–220	1.5–12.5
C and A–C trend	Early/late	Generally secondary	155–220	14.5–24.5

* = end member representative value.

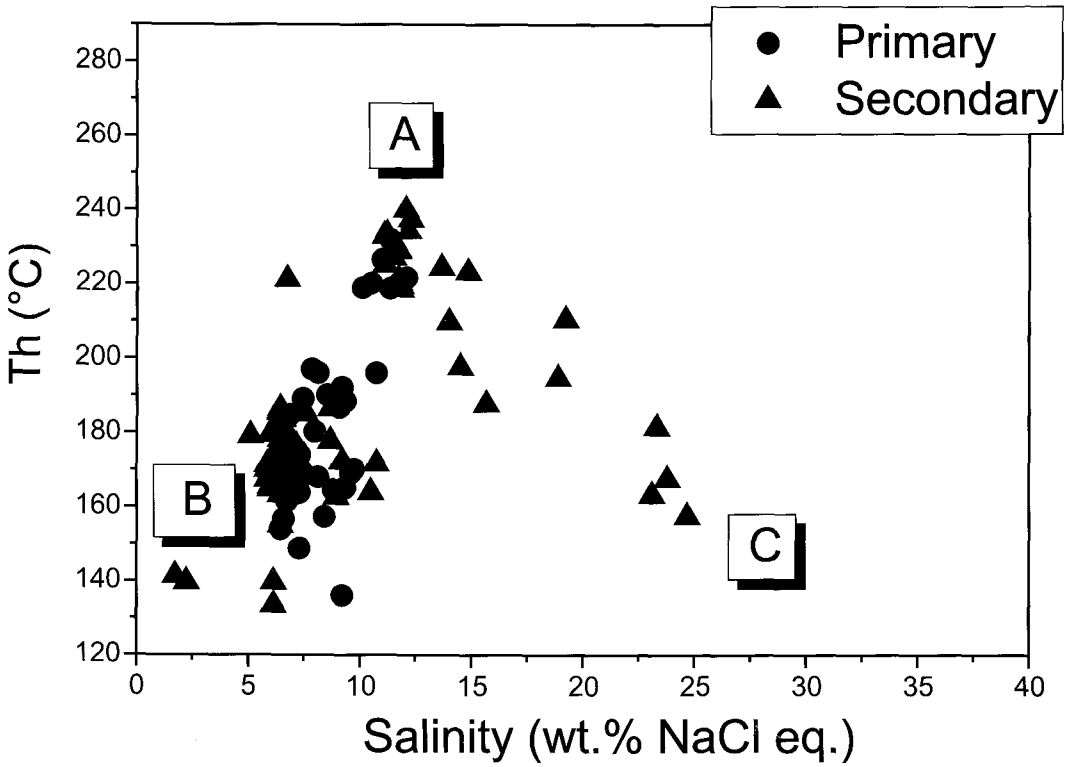

FIG. 3. Temperature of homogenization *vs.* salinity diagram for the studied inclusions. The letters indicate the three hypothetical end-member fluids. See text for explanations.

of the A–C array are secondary (Table 1). In a few cases, fluid inclusions having appreciably different salinities (from about 20 to 10 wt.% NaCl eq.) were found along the same trail.

Carbonate composition and geothermometry

The calcite–dolomite geothermometer, based on the Mg content of calcite in equilibrium with dolomite, has been widely employed for temperature estimates in metamorphosed carbonate rocks (Essene, 1983; Powell *et al.*, 1984; Pan and Fleet, 1992; Mumin and Fleet, 1995). Specifically, the Powell *et al.* (1984) calibration of the geothermometer in the $CaCO_3$-$MgCO_3$-$FeCO_3$ system at temperatures between 300 and 450°C usually yielded results consistent with independent temperature estimates (see Mumin and Fleet, 1995). Calcites from the AA marbles have negligible MnO and FeO contents (up to 0.11 and 0.70 wt.%, respectively (Table 2), low enough to allow the application of the calcite–dolomite geothermometry. MgO in analysed calcites varies between 0.07 and 1.15 wt.% (Table 2). The MgO content may be locally variable at the single grain scale, but no systematic compositional zoning was detected. The geothermometric estimates (Fig. 4) show that the early generation of calcite records temperatures predominantly between 300 and 400°C, whereas late calcites have very low MgO contents, leading to temperatures estimates generally lower than 300°C.

Discussion

Fluid source(s)

The trends shown in Fig. 3 may be interpreted as being the result of mixing of the three different end-member fluids: A, B and C. These fluids circulated during the greenschist-facies metamorphism of the AA area. This conclusion is supported by: (1) the vein structural setting, which is compatible with a syn-deformational and syn-

TABLE 2. Representative microprobe analyses (in wt.%) of early (E) and late (L) calcites. CO_2 has been calculated assuming stoichiometry

Sample E = early	GB 189 E	GB 182 E	GB 119 E	GB 121 E	GB 164 E	GB 163 E
CaO	55.25	55.51	55.33	54.38	53.88	54.58
MgO	0.65	0.94	0.93	0.97	1.15	0.78
FeO	0.09	BDL	BDL	0.05	0.05	BDL
MnO	BDL	BDL	BDL	BDL	0.07	BDL
SiO_2	0.05	BDL	0.06	0.14	BDL	BDL
CO_2	44.12	44.61	44.45	43.77	43.61	43.72
Total	100.16	101.06	100.77	99.31	98.76	99.08
Sample L = late	GB 182 L	GB 119 L	GB 189 L	GB 121 L	GB 164 L	GB 163 L
CaO	55.18	55.95	55.71	55.54	55.7	55.13
MgO	0.29	0.33	0.26	0.29	0.28	0.22
FeO	0.12	BDL	0.15	0.05	BDL	BDL
MnO	BDL	BDL	BDL	0.05	BDL	BDL
SiO_2	BDL	BDL	0.04	0.14	0.05	BDL
CO_2	43.69	44.28	44.09	43.97	44.03	43.51
Total	99.28	100.56	100.25	100.04	100.06	98.86

BDL: below detection limit.

metamorphic fluid infiltration (Kligfield *et al.*, 1986; Carmignani and Kligfield, 1990); (2) the agreement between trapping temperature and pressure estimated by the microthermometric data of primary inclusions (see below), with the *P–T* conditions of metamorphic peak in the AA (Kligfield *et al.*, 1986; Carmignani and Kligfield, 1990; Costagliola *et al.*, 1998); (3) the absence of post-entrapment reequilibration textures of these fluid inclusions. As far as the source of fluids is concerned, we must consider the hypothesis of a contribution from devolatilization reactions during prograde metamorphism of the host marble. However, the mineral assemblage of the Carrara marbles includes very limited amounts of hydrous silicates and of their possible metamorphic products, so that H_2O production was conceivably minimal. Moreover, fluid circulation in the studied veins occurred late in the tectonometamorphic history of the host marble, when presumably most of its capability of internal fluid generation was already used up. Finally, the widely different nature of the three supposed end-member fluids point to multiple sources. Pervasive fluid/rock interaction within the marble level may be ruled out. In fact, the $\delta^{18}O$ and $\delta^{13}C$ composition of marble calcite is remarkably homogeneous, and typical of a sedimentary environment (Cortecci *et al.*, 1985), with little evidence of isotopic shifts due to fluid circulation. The Marble formation, therefore, substantially behaved as an aquitard, and was a passive host to the metamorphic fluid circulation. Hence, the veins hosted by the Marble should have been formed by fluids originated largely in some external reservoir, either below and/or above the marble level, possibly channeled along the listric faults and shear zones which affected the core complex during its extensional stage (Carmignani and Kligfield, 1990).

Fluid inclusions very similar to fluid A have been frequently observed in the gangue phases (mostly quartz) of the metamorphogenic deposits hosted by the AA basement (Lattanzi *et al.*, 1994; Benvenuti *et al.*, 1995; Costagliola *et al.* 1998). These fluids are thought to have equilibrated with the volcano/sedimentary sequences of the basement. The source of fluid A could therefore be recognized in the lower levels of the NMA, possibly in the Palaeozoic basement.

Although the reliability of the calcite-dolomite geothermometer is limited to the highest tempera-

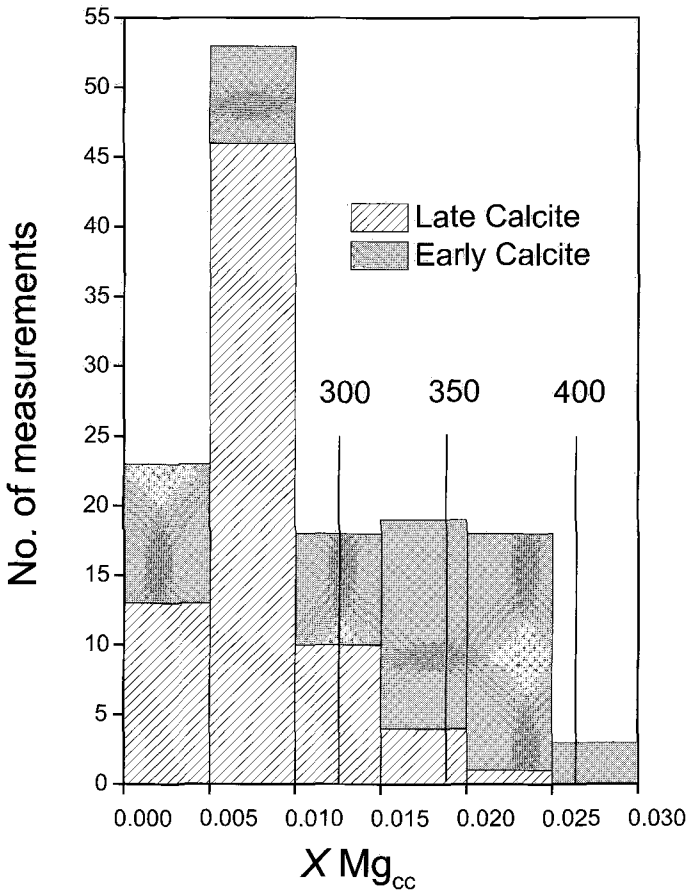

FIG. 4. Histograms showing the Mg content of calcites. Vertical lines indicate the temperature estimates obtained by applying the calibration of Powell *et al.* (1984).

ture estimates (around 400°C; cf. Essene, 1983), the general trend of decreasing Mg from early to late calcites suggests a temperature decrease with time (Fig. 4). This is in accordance with fluid inclusion data, showing a decrease of T_h from A to B/C. In particular, the low salinity and temperature of the fluid B is in marked contrast with all previous fluid inclusion data in the AA area, as reported by Lattanzi *et al.*, (1994). The general characteristics of fluid B match well those of a meteoric fluid, suggesting that the listric faults at high structural levels provided suitable conduits for fluid infiltration.

Fluid type C, although less well constrained due to the comparatively smaller amount of data, shows comparable T_h, but a distinctly higher salinity than fluid B. Fluids supersaturated or close to saturation in NaCl at room temperature are known in the AA basement (Lattanzi *et al.*, 1994). Textural and structural evidences suggest that these fluids postdate the main orogenic stage, and circulated during the uplift of the AA core complex. Recently, Hodgkins and Stewart (1994) described supersaturated fluid inclusions hosted in minerals cementing the window fault breccia, that is located just below the evaporitic level of the Tuscan Nappe, and above the Marble formation. These inclusions are thought to be samples of the syntectonic (syn-D_2) fluids channeled along the fault zone. Hodgkins and Stewart (1994) found evidence that these saline fluids were not reintroduced from the fault zone toward the underlying metamorphic rocks. However, taking into account that the *en-echelon* veins in the Carrara Marble are located not far from the detachment fault, the evaporitic levels at the base

of the Tuscan Nappe are seemingly the most obvious source for the saline fluids in the Marbles. As shown in Fig. 3, saline fluid inclusions are typically secondary. The crystal planes where they lie in may also host other inclusions having distinctly lower salinities. This could imply that changes in fluid composition occurred in a time span shorter than that required to seal the host mineral fractures. The cyclical expulsion from the fault breccia, following a fault-valve model (Sibson, 1992), of batches of saline fluids not completely mixed and homogenized with the dominant lower-salinity fluid, may account for this feature (cf. Fricke *et al.*, 1992).

Concerning the mechanisms of deposition of the numerous mineral species in marble veins, the mixing of different fluids may have had an important role. In fact, most of these minerals have solubilities decreasing with decreasing fluid salinity and/or cooling (Barnes, 1979; Holland and Malinin, 1979). The dominant mixing trend between fluid A and B suggests that the basement-derived fluids, probably carrying elements leached from the infiltrated rocks, deposited the minerals in the marble veins upon interaction with low-salinity, low-temperature, presumably oxidizing meteoric fluids.

Mixing and ore-forming processes in the Apuane Alps core complex

The formation of precious and base metal deposits associated with the detachment structures of metamorphic core complexes, is often related to the presence of two dominant fluid types: a high-temperature, moderately saline, metal-bearing fluid, isotopically equilibrated with metamorphic rocks, and a low-temperature, low-salinity, oxidizing meteoric fluid (Spencer and Welty, 1986; Beaudoin *et al.*, 1991; 1992). In this kind of deposit, fluid inclusion salinities and homogenization temperatures are between 0–20 wt.% NaCl eq. and 100–300°C, respectively (Beaudoin *et al.*, 1992; Smith *et al.*, 1991). It is widely accepted that high-angle normal faults in the Upper Plate, connected with detachment fault or shear zones in the Lower Plate, may provide suitable sites for the mixing of hydrothermal fluids of metamorphic origin with meteoric fluids, thus leading to the precipitation of metals. Fluid mixing, therefore, is a typical feature of the late stage of core complex development, and it is intimately associated with crustal extension (Beaudoin *et al.*, 1991; 1992; Kerrich, 1987; Kyser and Kerrich, 1990). By contrast, in the AA no evidence of fluid mixing was found either along the detachment fault (Hodgkins and Stewart, 1994) which is, indeed, completely barren, or in the shear zones cross-cutting the core complex, where, at opposite, economic ore deposits occur (see Lattanzi *et al.*, 1994 and literature therein). In other words, the penetration at depth of meteoric waters and their mixing with upwelling hydrothermal fluids was apparently a very limited phenomenon in the AA, being restricted mainly to minor structures such as the studied veins.

Crustal extension has been recently considered as a powerful driving force for fluid flow and mineral deposition (Ilchik and Barton, 1997). The development of a substantial hydrothermal activity and mineral deposition in extensional areas and, in particular, in core complexes, is usually ascribed to an increase of the geothermal gradient in the shallow levels of the crust due to the uplift of the Lower Plate rocks (Spencer and Welty, 1986; Doblas *et al.*, 1988; Moritz and Ghazban, 1996). Steeply dipping uplift paths in a $P-T$ space may provide such conditions (Holm *et al.*, 1989), and therefore it may be argued that the absence of an extensive hydrothermal circulation at shallow levels in the AA is a consequence of the uplift path of this area. An uplift path for the southern region of the AA has been recently proposed by Costagliola *et al.*, (1994; Fig. 5). This path is fairly coincident with the average isochores of fluids B and C, and of fluid inclusions hosted by minerals deposited in syn-D_2 extensional structures in the breccia fault (Hodgkins and Stewart, 1994). According to these authors, fluid inclusions in both quartz and calcite are neither imploded nor exploded, suggesting that the differential between internal and confining pressure was constantly rather low. After Sterner and Bodnar (1989), we can conclude that the $P-T$ path during uplift was roughly coincident with the B, C, and breccia fault isochores. This would imply, in addition, that the uplift path obtained for the southern AA may be representative for the whole AA region. However, Fig. 5 shows that there is a departure between the uplift path and the isochores calculated for the inclusions in early quartz (type A) and for those in minerals from the extension veins in the basement rocks (Pollone area: Costagliola *et al.*, 1998). The trapping conditions of the former (type A) inclusions may be estimated by the Mg-content of calcite associated with dolomite and early quartz. By assuming temperatures of about 400°C, a corresponding trapping pressure of

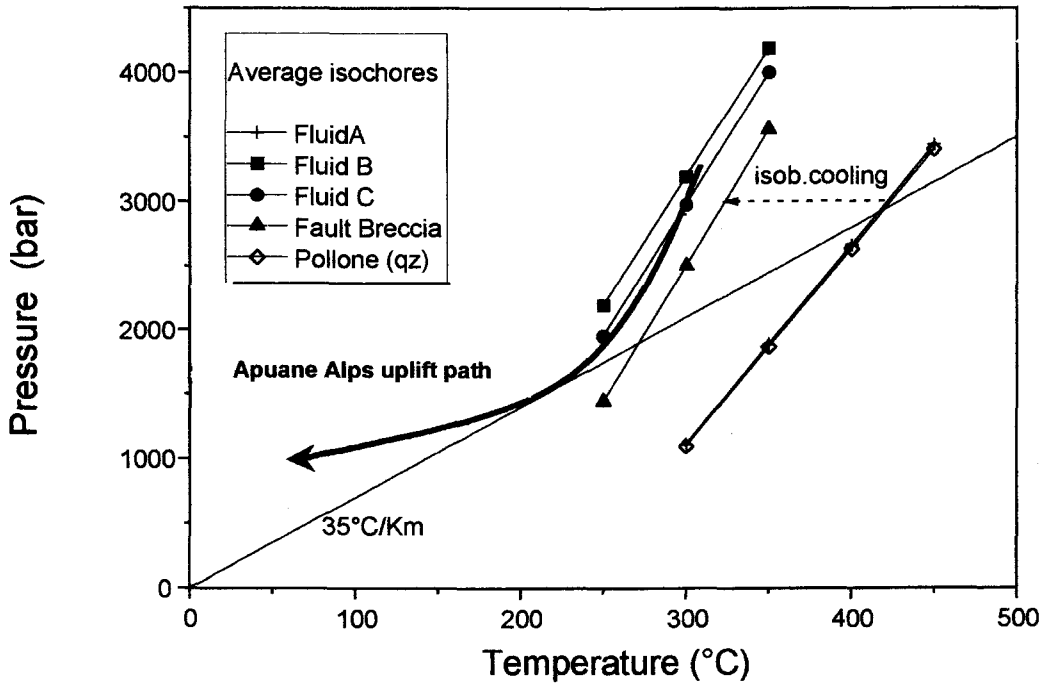

FIG. 5. Average isochores calculated in the present study (according to Zhang and Frantz, 1987) for fluids A, B and C, compared with those calculated by Hodgkins and Stewart (1994) for fluid inclusions in the detachment fault breccia, and by Costagliola *et al.* (1998) for fluid inclusions in extensional quartz veins of the Pollone deposit. The uplift path was drawn according to Costagliola *et al.* (1994).

about 3 kbar is obtained (Fig. 5). These $P-T$ conditions would represent the starting point for A and Pollone fluids. This system would have then experienced an almost isobaric cooling down to about 300°C (the temperature at which halite melts in the breccia fault's inclusions; Hodgkins and Stewart, 1994). Thermal reequilibration following isobaric cooling paths may result from the underthrusting of crustal segments (Thompson and England, 1984; Jawecki, 1996); however, in the AA this initial stage of cooling may simply reflect fluid cooling, rather than rock cooling. In fact, Costagliola *et al.* (1998) suggested that basement-derived fluids, similar to type A fluids, were adiabatically upraised through the crust. Hence, the observed cooling may simply indicate a thermal reequilibration between rocks and fluids. Notice that the maximum pressure difference between the proposed $P-T$ path and the isochore for fluid A is about 1.5 kbar. This is about the maximum value that fluid inclusions in quartz can withstand without undergoing deformation (Bodnar and Vityk, 1995).

The most rapid exhumation was experienced by the AA rocks between 3 and 1.5 kbar (Fig. 5), i.e. roughly the range of pressures (depths) at which the window fault was active (Hodgkins and Stewart, 1994). This range is in agreement with the amount of tectonic unroofing accomplished by extension (5–7 km), as estimated by Cello and Mazzoli (1996). This evidence suggests that the most rapid exhumation of the core complex was accomplished by extensional movements along the window fault, thus indicating a substantial degree of tectonic control on the cooling rate (cf. Ketcham, 1996). At the end of this stage, the AA area experienced the highest geothermal gradient, estimated to be about 35°C/km (see Fig. 5). This gradient is remarkably lower than documented in other core complexes with a mineralized detachment fault (up to about 100°C/km, see Spencer and Welty, 1986), where rapid uplift of metamorphosed terranes caused an intense circulation of meteoric waters that mixed with metamorphic fluids (Koons and Craw, 1991). The final stages of the uplift of the AA core complex

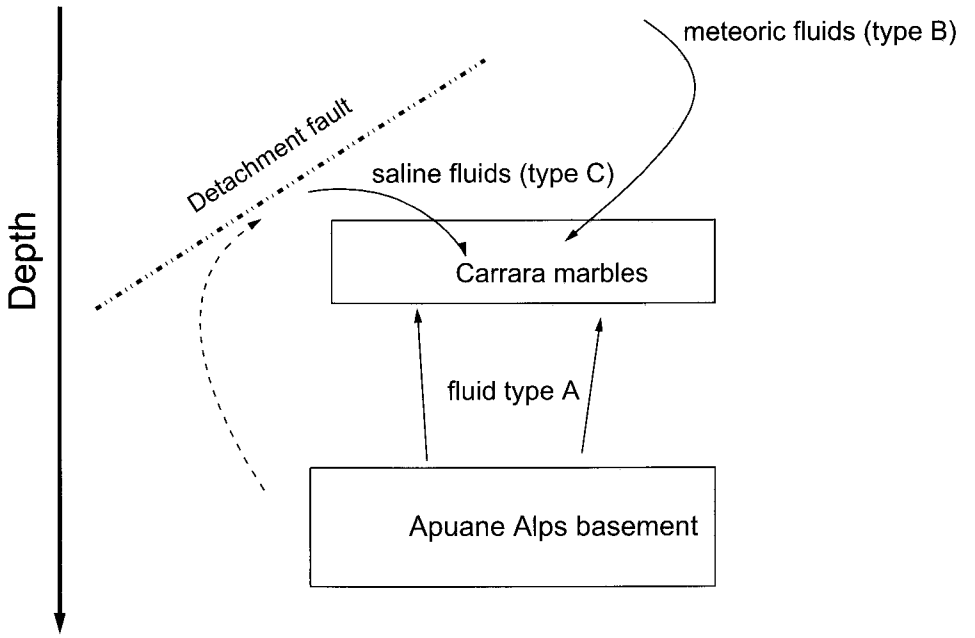

FIG. 6. Fluid circulation model in the Apuane Alps core complex. Dashed fluid path from Hodgkins and Stewart (1994).

were presumably characterized by erosion of the core complex, and subsequent rapid (isobaric) cooling of deep structural levels (cf. Hodgkins and Stewart, 1994). Isobaric cooling during the final stages of the uplift is rather common in other core complexes (Hill *et al.*, 1992; Ketcham, 1996). A possible mechanism invoked to explain this late $P-T$ trend is the existence of intense hydrothermal activity at shallow levels, since convection is a quite effective cooling mechanism (Holm *et al.*, 1989). However, in the AA there is no evidence of this, and it is more likely that the decrease of temperature was accelerated as the rocks approached the surface (see Ketcham, 1996), thus leading to an almost flat $P-T$ trajectory during the latest stages of exhumation.

Conclusions

Calcite–dolomite geothermometry and fluid inclusion data suggest that early fluids circulating in the veins of the Carrara marble had temperatures of about 400°C at pressures of about 3 kbar. These fluids were presumably of largely external origin, and may have been generated in the underlying Palaeozoic basement (Fig. 6). Mineral deposition in the veins was consequent to mixing of these 'deep' fluids with meteoric waters. Minor contributions to fluid circulation were represented by relatively saline fluids, equilibrated with evaporitic rocks located along the detachment fault of the AA core complex (Fig. 6). Fluid mixing is evident only in minor structures of the core complex (like the veins in the marbles), and not along the major tectonic structures, such as shear zones and the detachment fault, indicating that meteoric fluid ingression in the complex was rather limited. These features would markedly distinguish the hydrology of the AA with respect to other core complexes, where mixing and consequent ore deposition occurred along major extensional structures. Fluid inclusion constraints on the uplift path of the core complex indicate a tectonic control on the cooling rate. In fact, comparatively rapid unroofing was experienced for a short segment of the uplift trajectory, probably as a consequence of the activity of the window fault. However, a high geothermal gradient was never reached, hindering the establishment of hydrothermal activity at shallow level. As a consequence, mineralization related to mixing phenomena along major

extensional tectonic structures is not expected in this area.

Acknowledgements

Funds for this research were provided by the Museo di Mineralogia, Università di Firenze, and by the Consiglio Nazionale delle Ricerche. The authors wish to thank all the quarrying companies which allowed sampling in their properties, Gloria Vaggelli and Filippo Olmi for assistance with microprobe analyses, and Szabolcs Harangi and Rita Kovacs for their help in the field. We are indebted to Giovanni Bertotti, Ernst A.J. Burke, Curzio Cipriani, Fabio Rosso, and an anonymous reviewer for their helpful suggestions.

References

Barnes, H.L. (1979) The solubility and occurrence of non-ore forming minerals. In *Geochemistry of Hydrothermal Ore Deposits,* (H.L. Barnes, ed.). John Wiley and Sons, NewYork, 461–508.

Beaudoin, G., Taylor, B.E. and Sangster, D.F. (1991) Silver-lead-zinc veins, metamorphic core complexes, and hydrologic regimes during crustal extension. *Geology,* **19**, 1217–20.

Beaudoin, G., Taylor, B.E. and Sangster, D.F. (1992) Silver-lead-zinc veins and crustal hydrology during Eocene extension, southern British Columbia, Canada. *Geochim. Cosmochim. Acta,* **56**, 3513–29.

Benvenuti, M., Costagliola, P., Lattanzi, P. and Tanelli, G. (1995) The metamorphic hosted siderite-Cu deposit of Frigido: structural setting and isotopic data. In *Mineral Deposits: from their Origin to their Enviromental Impact* (J. Pasava, B. Kribek and K. Zak, eds), Balkema, Rotterdam, 843–6.

Bodnar, R.J. (1993) Revised equation and table for determining the freezing point depression of H_2O-NaCl solutions. *Geochim. Cosmochim. Acta,* **57**, 683–4.

Bracci, G., Dalena, D. and Orlandi, P. (1978) I geodi del marmo di Carrara. [Geodes of the Carrara marble]. *Atti Soc Tosc. Sci. Nat., Mem., XXIV Serie A,* **85**, 221–41.

Carmignani, L. and Kligfield, R. (1990) Crustal extension in the Northem Apennines: the transition from compression to extension in the Alpi Apuane core complex. *Tectonics,* **9**, 1275–303.

Carmignani, L., Fantozzi, P.L., Giglia, G., Kligfield, R. and Meccheri, M. (1992) Tettonica di crosta media e di crosta superiore nelle Alpi Apuane: un modello per l'interpretazione dei profili sismici a riflessione dell'Appennino settentrionale. [Middle and upper crustal tectonics in the Apuane Alps: a model for interpretation of seismic profiles in the northern Apennines]. *Studi Geologici Camerti,* Vol. Spec. **2**, CROP 1-1 A, 211–25.

Cello, G. and Mazzoli, S. (1996) Extensional processes driven by large-scale duplexing in collisional regimes. *J. Struct. Geol.,* **18**, 1275–9.

Cortecci,G., Lattanzi, P. and Tanelli, G. (1975) C and O-isotope and fluid inclusion studies of carbonate from pyrite and polymetallic ore deposits and associated country rocks (Southern Tuscany, Italy). *Chem. Geol-Isot. Geosci. sect.,* **58**, 121–8.

Costagliola, P., Benvenuti, M., Lattanzi, P. and Tanelli, G. (1994) Uplift path of metamorphic terranes in the Apuane Alps: evidence from fluid inclusion in the Pollone deposit. *Mem. Soc. Geol It.,* **48**, 719–23.

Costagliola, P., Barbieri, M., Benvenuti, M., Lattanzi P. and Castorina, F. (1995) Sr-isotope composition of barite veins at Pollone deposit, Apuane Alps, Tuscany, Italy. In *Mineral Deposits: from their Origin to their Enviromental Impact.* (J. Pasava, B. Kribek and K. Zak, eds) Balkema, Rotterdam, 341–4.

Costagliola, P., Benvenuti, M., Lattanzi, P. and Tanelli, G. (1998) Metamorphogenic barite-pyrite(Pb-Zn-Ag) veins at Pollone, Apuane Alps, Tuscany: vein geometry, geothermobarometry, fluid inclusions and geochemistry. *Mineral. Petrol.,* **62**, 29–60.

Crisci, A., Cipriani, C. and Costagliola, P. (1997) Nuovi dati sull'associazione mineralogica dei Marmi di Carrara, Alpi Apuane. [New data on mineral assemblage in the Carrara marble, Apuane Alps]. *Museol. Scient.,* **XIII**, 267–79.

Doblas, M., Oyarzun, R., Lunar, R., Mayor, N. and Martinez, J. (1988) Detachment faulting and late Paleozoic epithermal Ag-base-metal mineralization in the Spanish central system. *Geology,* **16**, 800–3.

Essene, E.J. (1983) Solid solution and solvi among metamorphic carbonates with applications to geologic thermobarometry. In *Carbonates – Mineralogy and Chemistry* (R.J. Reeder, ed.) *Rev. Mineral.,* **11**, 77–96.

Franzini, M., Orlandi P., Bracci, G. and Dalena, D. (1992) Mineralien der Marmors von Carrara. [Minerals of the Carrara Marble] *Mineralien Welt,* **3**, 16–46.

Fricke H.C., Wickham S.M. and O'Neil J.R. (1992) Oxygen and hydrogen isotope evidence for meteoric water infiltration during mylonitization and uplift in the Ruby Mountains-East Humboldt Range core complex, Nevada. *Contrib. Mineral. Petrol.,* **111**, 203–21

Hodgkins, M.A. and Stewart, K.G. (1994) The use of fluid inclusions to constrain fault zone pressure, temperature and kinematic history – an example from Alpi Apuane, Italy. *J. Struct. Geol.,* **16**, 85–96.

Hill, E.J., Baldwin, S.L. and Lister, G.S. (1992)

Unroofing of active metamorphic core complexes in the D'entrecasteaux Island, Papaua New Guinea, *Geology,* **20**, 907–10.

Holland, H.D. and Malinin, S.D. (1979) The solubility and occurrence of non-ore forming minerals. In *Geochemistry of Hydrothermal Ore Deposits, 2nd ed.* (H.L. Barnes, ed.). John Wiley and Sons, New York, 461–508.

Holm, D.K, Norris, R.J. and Craw, D. (1989) Brittle and ductile deformation in a zone of rapid uplift: central Southem Alps, New Zealand. *Tectonics,* **8**, 153–68.

Ilchik R.P. and Barton M.D. (1997) An amagmatic origin of Carlin-type gold deposits. *Econ. Geol.,* **92**, 269–88.

Jawecki, C. (1996) Fluid regime in the Austrian Moldanubian Zone as indicated by fluid inclusions. *Mineral. Petrol.,* **58**, 235–52.

Kerrich, R. (1987) Detachment zones of Cordilleran metamorphic core complexes: thermal fluid and metasomatic regimes. *Geol. Rundschau,* **77**, 157–82.

Ketcham, R.A. (1996) Thermal models of core complex evolution in Arizona and New Guinea: Implications for ancient cooling paths and present-day heat flow. *Tectonics*, **15**, 933–51.

Kligfield, R., Hunziker, J., Dallmeyer, R.D. and Schamel, S. (1986) Dating of deformation phases using K-Ar and $^{40}Ar/^{39}Ar$ techniques - results from Northern Apennines. *J. Struct. Geol.,* **8**, 781–98.

Kyser, T. and Kerrich R. (1990) Geochemistry of fluids in tectonically active crustal regions. In *Fluids in Tectonically Active Regimes of the Continental Crust,* (B.E. Nesbitt, ed.). *Min. Ass. Canada Short Course Handb.,* **18**, 133–230.

Koons, P.O. and Craw, D. (1991) Gold mineralization as a consequence of continental collision: an example from the Southern Alps, New Zealand. *Earth Plan. Sci. Lett.,* **103**, 1–9.

Lattanzi, P., Benvenuti, M., Costagliola, P. and Tanelli, G. (1994) An overview on recent research on the metallogeny of Tuscany, with special reference to the Apuane Alps. *Mem. Soc. Geol It.,* **48**, 613–25.

Moritz, R. and Ghazban, F. (1996) Geological and fluid inclusion studies in the Muteh gold district, sanandaj-Sirjan zone, Isfahan Province, Iran. *Schweiz. Mineral. Petogr. Mitt.,* **76**, 85–9.

Mumin, A.H. and Fleet, M.E. (1995) Evolution of gold mineralization in the Ashanti Gold Belt, Ghana: evidence from carbonate composition and paragenesis. *Mineral. Petrol.,* **55**, 265–80.

Orlandi, P., Del Chiaro, L. and Pagano, R. (1996) Minerals of the Seravezza Marble, Tuscany, Italy. *Mineral. Record,* **27**, 47–58.

Pan, Y. and Fleet, M.E. (1992. Calc-silicate alteration in the Hemlo gold deposit Ontario: mineral assemblages, P-T-X constraints and significance. *Econ. Geol.,* **87**, 1104–21,

Powell, R., Condliffe, D.M. and Condliffe, E. (1984) Calcite-dolomite geothermometry in the system $CaCO_3$-$MgCO_3$-$FeCO_3$ – an experimental study. *J. Metam. Geol.,* **2**, 33–41.

Sibson, R.H. (1992) Implications of fault valve behaviour for rupture nucleation and recurrence. *Tectonophysics,* **211**, 283–93.

Smith, B.M., Reynolds, S.J., Day, H.W. and Bodnar, R.J. (1991) Deep-seated fluid involvement in ductile-brittle deformation and mineralization, South Mountains core cornplex, Arizona. *Geol. Soc. Amer. Bull.,* **103**, 559–69.

Spencer, J.E. and Welty, J.W. (1986) Possible controls of base- and precious-metal mineralization associated with Tertiary detachment faults in the lower Colorado River trough, Arizona and California. *Geology,* **14**, 195–8.

Sterner, S.M and Bodnar, R.J. (1989) Synthetic fluid inclusions – VII. Re-equilibration of iluid inclusions in quartz during laboratory-simulated metamorphic burial and uplift. *J. Metam. Geol.,* **7**, 243–60.

Thompson, A.B. and England, P.C. (1984) Pressure temperature time paths of regional metamorphism: their inference and interpretation using mineral assemblages in metamorphic rocks. *J. Petrol.,* **25**, 929–55.

Vityk, M.O. and Bodnar, R.J. (1995) Do fluid inclusions in high-grade metamorphic terranes preserve peak metamorphic density during retrograde compression? *Amer. Mineral.,* **80**, 641–4.

Zhang, Y.G. and Frantz, J.D. (1987) Determination of the homogenization temperatures and densities of supercritical fluids in the system NaCl-KCl-$CaCl_2$-H_2O using synthetic fluid inclusions. *Chem. Geol.,* **74**, 289–308.

[*Manuscript received 12 December 1997: revised 16 June 1998*]